Journal of Marine Research, *55*, 735–766, 1997

Propagation of near-inertial oscillations through a geostrophic flow

by W. R. Young[1] and Mahdi Ben Jelloul[1]

ABSTRACT

The method of multiple time scales is used to obtain an approximate description of the linear propagation of near-inertial oscillations (NIOs) through a three-dimensional geostrophic flow. This 'NIO equation' uses a complex field, $M(x, y, z, t)$, related to the demodulated horizontal velocity by $M_z = \exp(if_0t)(u + iv)$, where f_0 is the inertial frequency. The three processes of wave dispersion, advection by geostrophic velocity and refraction (geostrophic vorticity slightly shifts the local inertial frequency) are all included in the formulation. The NIO equation has an energy conservation law, so that there is no transfer of energy between NIOs and the geostrophic flow in the approximation scheme.

As an application, the NIO equation is used to examine propagation of waves through a field of smaller scale, geostrophic eddies. The spatially local $\zeta/2$ frequency shift, identified by earlier WKB calculations (ζ is the vertical vorticity of the geostrophic eddies), is not expressed directly in the wave field: the large-scale NIO samples regions of both positive and negative ζ so that there is cancellation. Instead, the $\zeta/2$ frequency shift is rectified to produce an average dispersive effect. The calculation predicts that an NIO with infinite horizontal scale has a frequency shift $-Kf_0m^2/N^2$ where K is average kinetic energy density of the geostrophic eddies, m the vertical wavenumber of the NIO, f_0 the inertial frequency and N the buoyancy frequency. Because of the dependence of the frequency shift on m^2, there is an effective vertical dispersion, whose strength is proportional to the eddy kinetic energy. This process greatly increases the vertical propagation rate of synoptic scale NIOs.

1. Introduction

Near-inertial oscillations (NIOs) are excited by the large scale wind-stress exerted on the ocean by the atmosphere. This ringing is one of the most easily observed oscillations in the ocean: the inertial peak of the internal wave spectrum contains about half the total kinetic energy of the ocean, and an even larger fraction of the mean square vertical shear. Vertically propagating NIOs escape from the base of the mixed layer into regions where the buoyancy frequency is weaker. Thus, the NIO shear might reduce the Richardson number below ¼ and trigger mixing events. It is a widely received opinion that this is a significant mechanism for mixing the upper ocean.

A problem with the scenario described above is that that NIOs with small horizontal wavenumbers propagate extremely slowly. Gill (1984) estimated that an NIO with a

1. Scripps Institution of Oceanography, University of California at San Diego, La Jolla, California, 92093-0230, U.S.A.

horizontal scale of 1000 km (typical of the atmospheric forcing mechanism) will radiate out of the mixed layer on time scales of one year or longer. For instance, an NIO with a horizontal wavelength of 500 km, a vertical wavelength of 100 m, propagating in a fluid with $N = 10^{-2}\ s^{-1}$ and $f = 10^{-4}\ s^{-1}$, has a vertical group velocity of about 5 cm/day. This prediction is at odds with observations that, after a storm, NIO activity in the mixed layer returns to background levels in about 20 days (D'Asaro *et al.*, 1995). The concurrent observation of a vertically radiating "beam" of NIOs suggests that wave propagation is responsible for this decay. The implied propagation rate is about 10 meters per day—a factor of 200 times faster than the estimate above.

It is possible that this disparity is related to an earlier puzzle: the 10 km horizontal coherence scale of NIOs is much smaller than the 1000 km scale of atmosperic forcing. A plausible hypothesis is that, although inertial oscillations are initially forced with a large horizontal scale, advective distortion by mesoscale eddies decreases the NIO coherence scale (Weller, 1982).

These observations provide an incentive to better understand near-inertial dynamics, with an emphasis on the role of the mesoscale eddy field. This paper develops an approximation isolating the near-inertial part of internal wave dynamics. The approximation has three advantages over alternative strategies, such as WKB and numerical integration (e.g., Klein and Treguier, 1995; Kunze, 1985; Rubenstein and Roberts, 1986; Wang, 1991), which have been used in the past:

(i) The approximation avoids the vertical normal mode representation.

(ii) The approximation "filters" the $\exp(-if_0t)$ oscillation and leaves the subinertial changes.

(iii) The approximation does not make spatial scale separation assumptions.

As far as point (i) is concerned, it is obvious that vertical normal modes, used by Pollard (1970) and Gill (1984), are an inefficient means of representing a spatially compact inertial disturbance in the upper ocean (see, for example, the remarks on Poisson summation in Kloosterziel and Müller, 1995). Further, modeling a realistic environment requires the inclusion of vertically sheared geostrophic currents and their associated "thermal-wind" density structure. In this case, the linearized equations of motion are no longer separable and the projection onto vertical normal modes is problematic.

Turning to point (ii), numerical studies of NIOs using the full equations of motion have a time step limitation imposed by the necessity of resolving inertial cycles. Yet the interesting evolution takes place on longer time scales. A filtering approximation, isolating the slow subinertial evolution of NIOs, and relieving the computer from the responsibility of tracking predictible oscillations, is desirable. Then computational resources can be focussed on the interesting part of the problem.

Concluding with point (iii): because NIOs are generated by atmospheric forcing on scales of 1000 km one must be concerned with the case in which the length scale of the NIO greatly exceeds the length scale of the mesoscale eddy field (say 40 km). On the other hand, validity of the WKB approximation, used, for instance, by Kunze (1985), requires that the wavelength of the NIOs be somewhat smaller than the horizontal length scale of the eddies. Thus, conclusions based on ray tracing are not compelling because the "small" parameter in the WKB expansion is around 25. An advantage of the approximations developed in this article is that they provide an analytic avenue into the class of realistic problems in which NIOs propagate through an "effective medium" of small scale, geostrophic eddies. At the same time, since there is no assumption of scale separation in either direction, the approximation can recover the WKB limit.

In Section 2 we formulate the problem of linear NIOs superposed on a geostrophic flow. A multiple time-scale expansion is used to obtain a reduced description of NIO dynamics. Section 3 discusses the different processes described by this NIO equation.

A major part of Sections 2 and 3 is concerned with a careful multiple time expansion. These necessary calculations are technical because of the assumption that the vertical length scale of the geostrophic flow is comparable to that of the NIO. One consequence of this approach is that the simplicity of the approximation may be obscured for some readers. Fortunately, in most cases of oceanographic interest, the geostrophic flow has a larger vertical length scale than that of the NIO. Exploiting this scale separation produces further simplifications; this reduction is the goal of Section 4.

Probably the most generally useful result in this paper is an approximation developed in Section 4, and written in terms of a complex field, $A(x, y, z, t)$. The demodulated velocity of the NIO is related to A by

$$u + iv = e^{-if_0 t}[(f_0/N)^2 A_z]_z. \tag{1.1}$$

One can visualize the complex scalar A as a two-dimensional vector at each point in space. Eq. (1.1) can be used to compute the demodulated NIO velocity by differentiating A. The other NIO fields, such as the pressure and buoyancy, are obtained from A by differentiating with respect to the horizontal coordinates.

Defining $LA \equiv [(f_0/N)^2 A_z]_z$, and using other standard notation, introduced systematically below, the evolution equation from Section 4 is

$$LA_t + \frac{\partial(\Psi, LA)}{\partial(x, y)} + \frac{i}{2} f_0 \nabla^2 A + i\left(\beta y + \frac{1}{2}\nabla^2\Psi\right) LA = 0. \tag{1.2}$$

The second, third and fourth terms in (1.2) are, respectively, advection, dispersion and refraction of the near-inertial waves. Both the NIO equation from Section 2, and the simplified version in (1.2), have an energy conservation law; to leading order there is no transfer of energy between the NIO and the geostrophic flow.

In Section 5 we use the NIO equation to study the propagation of large horizontal scale NIOs through a field of small horizontal scale eddies. This calculation identifies a mechanism that might be responsible for the rapid decay of near-inertial shear and energy in the mixed layer. Section 6 is the conclusion and discussion.

2. Derivation of a reduced equation

a. Formulation. Consider an NIO propagating through a geostrophic flow. The geostrophic fields can be derived from a stream function, $\Psi(x, y, z, t)$. Thus, the geostrophic velocity and buoyancy fields are

$$(U, V, W, B) = (-\Psi_y, \Psi_x, 0, f_0\Psi_z). \tag{2.1}$$

The NIO propagates through the geostrophic background flow in (2.1). The total density field is decomposed as

$$\rho = \rho_0\left[1 - g^{-1}\int_0^z N^2(z')\,dz' - g^{-1}f_0\Psi_z - g^{-1}b\right], \tag{2.2}$$

where $b(x, y, z, t)$ is the buoyancy perturbation associated with the NIO. We assume that the interaction of the NIO with the geostrophic flow is described by the linearized and hydrostatic equations of motion

$$\begin{aligned}
\frac{Du}{Dt} + uU_x + vU_y + wU_z - fv &= -p_x,\\
\frac{Dv}{Dt} + uV_x + uV_y + wV_z + fu &= -p_y,\\
0 &= -p_z + b,\\
u_x + v_y + w_z &= 0,\\
\frac{Db}{Dt} + uB_x + vB_y + w(N^2 + B_z) &= 0,
\end{aligned} \tag{2.3a–e}$$

where the linearized convective derivative is

$$\frac{D}{Dt} = \partial_t + U\partial_x + V\partial_y. \tag{2.3f}$$

In (2.3), $f = f_0 + \beta y$ and $N(z)$ is the buoyancy frequency (or resting stratification) of a motionless fluid.

b. The scaling assumptions. Our goal is to obtain a reductive approximation of (2.3) using the assumption that the internal waves are nearly inertial. Thus, if λ_H is the horizontal wavelength, and λ_V is the vertical wavelength of the NIO, then we assume that the nondimensional parameter

$$\epsilon \equiv \frac{N_0\lambda_V}{f_0\lambda_H}, \tag{2.4}$$

is small. The constant N_0 in (2.4) is a scale factor for the buoyancy profile $N(z)$. A cautious definition is that N_0 is the maximum value of $N(z)$. From the internal wave dispersion relation, $\omega - f_0 = O(\epsilon^2 f_0)$. This means that the departures from perfect inertial oscillations become appreciable when $t \sim 1/\epsilon^2 f_0$ and we anticipate that

$$t_2 \equiv \epsilon^2 f_0 t, \tag{2.5}$$

is the appropriate "slow time scale."

Nondimensional coordinates, denoted with ^, are

$$(x, y) = \lambda_H(\hat{x}, \hat{y}), \qquad z = \lambda_V \hat{z}, \qquad \hat{t} = f_0 t. \tag{2.6a, b, c}$$

The independent variables are

$$(u, v) = f_0 \lambda_H(\hat{u}, \hat{v}), \qquad w = f_0 \lambda_V \hat{w}, \qquad b = N_0^2 \lambda_V \hat{b}, \qquad p = \epsilon^2 f_0^2 \lambda_H^2 \hat{p}. \tag{2.7a–d}$$

The most important choice made in defining the dimensionless variables in (2.6) and (2.7) is the ϵ^2 in the definition of $\hat{p}$. This ensures that the pressure gradient does not appear at leading order in the expansion.

The nondimensional β parameter is

$$\hat{\beta} = \frac{\beta \lambda_H}{\epsilon^2 f_0}. \tag{2.8}$$

The inertial frequency is $f = f_0(1 + \epsilon^2 \hat{\beta} \hat{y})$ and the variation of f over one horizontal wavelength is comparable to the dispersive correction of the NIO frequency, $\omega - f_0 = O(\epsilon^2 f_0)$.

We must also nondimensionalize the geostrophic fields in (2.3). We suppose that the function Ψ has the form

$$\Psi(x, y, z, t) = \epsilon^2 f_0 \lambda_H^2 \hat{\Psi}\left(\frac{x}{\lambda_H}, \frac{y}{\lambda_H}, \epsilon^q \frac{z}{\lambda_V}, \epsilon^2 f_0 t\right). \tag{2.9}$$

The scaling in (2.9) implies that the scale of the geostrophic velocity is $U_G \equiv \epsilon^2 f_0 \lambda_H$. Thus, the Rossby number, $Ro = U_G/\lambda_H f_0$, is equal to ϵ^2. The timescale of evolution in (2.9) is the slow time in (2.5) and this is consistent with the usual quasi-geostrophic time scale, Ro/f_0. The Doppler shift of the NIO frequency, of order U_G/λ_H, is also $O(\epsilon^2 f_0)$. Thus the NIO dispersive time scale, the quasigeostrophic time scale and the Doppler advection time scale are all of the same order.

For the scale of vertical variation of Ψ in (2.9) we have used λ_V/ϵ^q. The variable exponent, q, will be used to investigate the consequences of different assumptions concerning the strength of the geostrophic, vertical shear. The choice $q = 0$ makes the vertical scale of the geostrophic flow identical to that of the NIO. In this case the geostrophic buoyancy, $f_0\Psi_z$, is very strong: usually the vertical scale of geostrophic currents is greater than the vertical wavelength of NIOs.[2]

To weaken the geostrophic shear, one takes $q \geq 1$. For instance, the choice $q = 1$ makes the 'vortex stretching' contribution to the quasi-geostrophic potential vorticity, $(f_0^2N^{-2}\Psi_z)_z$, comparable to the 'relative vorticity', $\Psi_{xx} + \Psi_{yy}$. This is the usual quasigeostrophic scaling.

The Richardson number of the geostrophic flow in (2.9) is $Ri \equiv N^2/\Psi_{yz}^2 \sim \epsilon^{-2q-2}$. Because we are limiting attention to $q \geq 0$ the Richardson number of the background flow is well above the Miles-Howard threshold for stratified shear flow instability.

With the definitions above, the nondimensional, geostrophic velocity and buoyancy fields are

$$(\hat{U}, \hat{V}, \hat{B}) \equiv (-\hat{\Psi}_{\hat{y}}, \hat{\Psi}_{\hat{x}}, \hat{\Psi}_{\hat{z}}). \tag{2.10}$$

We now lighten the notation by dropping all the hats. The nondimensional version of (2.3) is then

$$\begin{aligned}
\frac{Du}{Dt} + \epsilon^2 uU_x + \epsilon^2 vU_y + \epsilon^{2+q} wU_z - (1 + \epsilon^2\beta y)v &= -\epsilon^2 p_x, \\
\frac{Dv}{Dt} + \epsilon^2 uV_x + \epsilon^2 vV_y + \epsilon^{2+q} wV_z + (1 + \epsilon^2\beta y)u &= -\epsilon^2 p_y, \\
0 &= -p_z + b, \\
u_x + v_y + w_z &= 0, \\
\frac{Db}{Dt} + \epsilon^q uB_x + \epsilon^q vB_y + w(N^2 + \epsilon^{2q}B_z) &= 0.
\end{aligned} \tag{2.11a–e}$$

The nondimensional convective derivative in (2.11) is

$$\frac{D}{Dt} = \partial_t + \epsilon^2[\partial_{t_2} + U\partial_x + V\partial_y], \tag{2.12}$$

where the slow time in (2.5) has been used to split the convective derivative into fast and slow components.

Notice how the parameter q appears in (2.11): all of the z derivatives that act on geostrophic fields are of order ϵ^q. For instance, in (2.11e), the term $B_z = \Psi_{zz}$ is multiplied by ϵ^{2q}.

2. The parameter ϵ^2 is the Burger number. Taking $q = 0$ means that the NIO and the geostrophic flow share the same, small Burger number. Geostrophic flows often have Burger numbers of order unity: this is the usual quasi-geostrophic assumption. But there are observations, particularly in the upper ocean, of geostrophic flows with small vertical scales and, presumably, small Burger number. Thus it is useful to first consider the case $q = 0$, and then retreat to easier scalings, such as $q \geq 1$.

The algebra is simplified if one uses the complex variables

$$\mathcal{U} \equiv u + iv, \tag{2.13a}$$

and

$$\xi \equiv x + iy. \tag{2.13b}$$

The spatial derivatives can be expressed in terms of ξ and ξ^* using

$$\partial_\xi = \tfrac{1}{2}[\partial_x - i\partial_y], \qquad \partial_{\xi^*} = \tfrac{1}{2}[\partial_x + i\partial_y], \tag{2.14a, b}$$

and the horizontal Laplacian and Jacobian are

$$\nabla^2 = 4\partial_\xi\partial_{\xi^*}, \qquad \frac{\partial(\xi, \xi^*)}{\partial(x, y)} = -2i. \tag{2.14c, d}$$

Using this notation, the horizontal momentum equations (2.11a, b) are

$$\mathcal{U}_t + i\mathcal{U} = -\epsilon^2 R, \tag{2.15a}$$

where

$$R = \mathcal{U}_{t_2} + \frac{\partial(\Psi, \mathcal{U})}{\partial(x, y)} + 2p_{\xi^*} + i\left[\beta y + \frac{1}{2}(\Psi_{xx} + \Psi_{yy})\right]\mathcal{U} + 2i\Psi_{\xi^*\xi^*}\mathcal{U}^* + 2iw\epsilon^q B_{\xi^*}. \tag{2.15b}$$

c. The choice $q = 0$. We now make the assumption that $q = 0$. With this choice, only even powers of ϵ appear in (2.11) and an approximate solution can be obtained by expanding in powers of ϵ^2 e.g., $\mathcal{U} = \mathcal{U}_0 + \epsilon^2\mathcal{U}_2 + \cdots$. In Section 4 we return and discuss the consequences of alternative scaling assumptions such as $q = 1$ and $q = 2$.

d. Terms of order ϵ^0. The leading order terms in (2.11) and (2.15) are

$$\begin{aligned} \mathcal{U}_{0t} + i\mathcal{U}_0 &= 0, \\ 0 &= -p_{0z} + b_0, \\ u_{0x} + v_{0y} + w_{0z} &= 0, \\ b_{0t} + u_0 B_x + v_0 B_y + w_0(N^2 + B_z) &= 0. \end{aligned} \tag{2.16a–d}$$

It is convenient to write the solution of (2.16a) as

$$\mathcal{U}_0 = M_z e^{-it}, \tag{2.17}$$

where $M(x, y, z, t_2)$ is a complex function.

The form in (2.17) makes it easy to solve (2.16) for w_0 and b_0. Integrating the mass conservation equation (2.16c) gives

$$w_0 = -M_\xi e^{-it} + \text{c.c.} \tag{2.18}$$

where "c.c." denotes complex conjugate. Because the vertical velocity is zero at the top ($z = 0$) and bottom ($z = -H$) of the ocean, M satisfies the boundary conditions

$$M(x, y, 0, t_2) = M(x, y, -H, t_2) = 0. \tag{2.19}$$

Eq. (2.19) also implies that the horizontal velocities in (2.17) have zero vertical average so that the barotropic mode of the NIO has been filtered.

The leading order buoyancy field, obtained from (2.16d), is

$$b_0 = i\frac{\partial(M, \tilde{B})}{\partial(\xi, z)} e^{-it} + \text{c.c.}, \qquad \tilde{B} \equiv \int_0^z N^2(z')\, dz' + B. \tag{2.20a, b}$$

The variable $\tilde{B}(x, y, z, t)$ is the total (resting plus geostrophic) buoyancy.

In principle, p_0 is obtained by integrating the hydrostatic relation in (2.16b). Writing

$$p_0 = Pe^{-it} + \text{c.c.} \tag{2.21}$$

one has

$$P_z = i\frac{\partial(M, \tilde{B})}{\partial(\xi, z)}. \tag{2.22}$$

Technical details of this integration, associated with the constant of integration in (2.22), are discussed in Appendix A. The point is that all of the leading order field can be obtained from the single complex function M.

e. Terms of order ϵ^2. At order ϵ^2, the horizontal momentum equations in (2.15) are

$$\mathcal{U}_{2t} + i\mathcal{U}_2 = -R_0, \tag{2.23}$$

where R_0 is obtained by inserting the leading order fields into (2.15b). R_0 contains resonant terms, proportional to exp $(-it)$, and nonresonant terms, proportional to exp (it). Eliminating the resonant terms gives the evolution equation for M. To perform this elimination it is convenient to first take the z-derivative of (2.23) and require that all the terms proportional to e^{-it} in R_{0z} cancel. This prescription produces

$$M_{zzt_2} + \frac{\partial(\Psi, M_{zz})}{\partial(x, y)} + i\left(\beta y + \frac{1}{2}\nabla^2\Psi\right)M_{zz} + \frac{i}{2}(N^2 + \Psi_{zz})\nabla^2 M - 4i\Psi_{z\xi}M_{z\xi^*} = 0. \tag{2.24}$$

Eq. (2.24) ensures that the z-derivative of (2.23) has no secularity. We must also separately consider the vertical average of (2.23) and ensure that there are no secular terms in this equation: details are in Appendix A.

We conclude this section by recording the solution of (2.23):

$$\mathscr{U}_2 = \left[iP^*_{\xi^*} + \frac{\partial(M^*, \Psi_{\xi^*})}{\partial(\xi^*, z)} \right] e^{it}. \tag{2.25}$$

Notice that $\mathscr{U}_0$ in (2.17) and $\mathscr{U}_2$ in (2.25) are proportional to $\exp(-it)$ and $\exp(it)$ respectively. The combination $\mathscr{U}_0 + \epsilon^2 \mathscr{U}_2$ produces the slightly elliptical hodograph characteristic of NIOs.

3. Discussion of the NIO approximation

We begin by summarizing the results of Section 2 in dimensional variables. The leading order fields of the NIO are obtained from the complex function **M** by:

$$\begin{aligned} u_0 + iv_0 &= M_z e^{-if_0 t}, \\ w_0 &= -M_\xi e^{-if_0 t} + \text{c.c.}, \\ b_0 &= \frac{i}{f_0}\frac{\partial(M, \tilde{B})}{\partial(\xi, z)} e^{-if_0 t} + \text{c.c.}, \\ p_0 &= \mathbf{P} e^{-if_0 t} + \text{c.c.} \end{aligned} \tag{3.1a–d}$$

where $\tilde{B} = \int_0^z N^2\, dz + f_0 \Psi_z$ is the total buoyancy (resting stratification plus geostrophic disturbance).

The dimensional version of Eq. (2.24) can be written in terms of conventional vector operators as

$$\begin{aligned} &M_{zzt} + \left[\frac{\partial(\Psi, M_z)}{\partial(x, y)}\right]_z + \frac{i}{2}[\![\tilde{\Psi}, M]\!] = 0, \\ &[\![\tilde{\Psi}, M]\!] \equiv \nabla \cdot (\tilde{\Psi}_{zz} \nabla M) - (\nabla \tilde{\Psi}_z \cdot \nabla M)_z - \nabla \cdot (\nabla \tilde{\Psi}_z M_z) + (\nabla^2 \tilde{\Psi} M_z)_z, \end{aligned} \tag{3.2a,b}$$

where $\nabla \equiv (\partial_x, \partial_y)$ is the two-dimensional gradient and

$$\tilde{\Psi} \equiv \frac{1}{3}\beta y^3 + \frac{1}{f_0}\int_0^z (z - z')N^2(z')\, dz' + \Psi. \tag{3.3}$$

The function $\tilde{\Psi}$ in (3.3) is defined so that $\nabla^2 \tilde{\Psi} = 2\beta y + \nabla^2 \Psi$ and $\tilde{\Psi}_{zz} = f_0^{-1} N^2 + \Psi_{zz}$.

The bracket product in (3.2) has a useful symmetry: taking the first two terms on the right-hand side of (3.2b) and exchanging the differential operators ∂_z and ∇ produces the second two terms. There are also several alternative forms of the bracket which are sometimes useful:

$$\begin{aligned} [\![\tilde{\Psi}, M]\!] &= \tilde{\Psi}_{zz} \nabla^2 M - 2\nabla \tilde{\Psi}_z \cdot \nabla M_z + \nabla^2 \tilde{\Psi} M_{zz}, \\ &= \nabla^2(\tilde{\Psi}, M_{zz}) - 2\nabla \cdot (\tilde{\Psi} \nabla M_z)_z + (\tilde{\Psi} \nabla^2 M)_{zz} \\ &= \nabla^2(M \tilde{\Psi}_{zz}) - 2\nabla \cdot (M \nabla \tilde{\Psi}_z)_z + (M \nabla^2 \tilde{\Psi})_{zz}. \end{aligned} \tag{3.4a, b, c}$$

The expressions in (3.4) show that $[\![\tilde{\Psi}, M]\!] = [\![M, \tilde{\Psi}]\!]$—a fact which is not immediately apparent from the definition in (3.2b). The main advantage of the form in (3.2b) is that it makes the closest contact between $[\![\tilde{\Psi}, M]\!]$ and the structure one has in a self-adjoint differential operator acting on M. This proves to be useful in the manipulations which arise in the course of proving that (3.2a) conserves energy.

a. Energy conservation equation. The NIO-equation, (3.2a), has an energy conservation law which is obtained by forming the combination M^* (3.2a) + M (3.2a)*. Following this prescription one eventually arrives at

$$E_t + \frac{\partial(\Psi, E)}{\partial(x, y)} + \nabla \cdot \mathbf{F} + G_z = 0, \tag{3.5}$$

where the energy density is

$$E \equiv \tfrac{1}{2} M_z M_z^*. \tag{3.6}$$

The flux in (3.5) is

$$\mathbf{F} = \frac{i}{4} \nabla \tilde{\Psi}_z (M^* M_z - M M_z^*) - \frac{i}{4} \tilde{\Psi}_{zz} (M^* \nabla M - M \nabla M^*),$$

$$G = \frac{i}{4} \nabla \tilde{\Psi}_z \cdot (M^* \nabla M - M \nabla M^*) - \frac{i}{4} \nabla^2 \tilde{\Psi} (M^* M_z - M M_z^*) \tag{3.7a, b}$$

$$- \frac{1}{2} \left(M^* \frac{DM_z}{Dt} + M \frac{DM_z^*}{Dt} \right),$$

where $\tilde{\Psi}$ is defined in (3.3).

According to Bretherton and Garrett (1968) the action, (energy density)/(intrinsic frequency), is conserved. But for NIOs, the intrinsic frequency is, to leading order, f_0. Thus, the action density is proportional to the energy density in (3.6). Consequently, with the scaling of this paper, (3.5) is both energy and action conservation.[3] The conservation law (3.5) shows that, at the order of (3.2), there is no transfer of energy between NIOs and geostrophic flow.

b. Special case: a barotropic current. We can develop some confidence in the NIO equation (3.2) by considering special cases and discussing the physical significance of the various terms. Begin by considering a barotropic flow i.e., $\Psi_z = 0$. With this simplification, (3.2) collapses to

$$M_{zzt} + \frac{\partial(\Psi, M_{zz})}{\partial(x, y)} + \frac{i}{2} \frac{N^2}{f_0} \nabla^2 M + i \left(\beta y + \frac{1}{2} \nabla^2 \Psi \right) M_{zz} = 0. \tag{3.8}$$

3. For NIOs the potential energy is negligible at leading order. Thus the energy in (3.6) is only kinetic.

The second, third and fourth terms on the left-hand side of (3.8) represent advection, dispersion and refraction respectively.

The advective term, $\partial(\Psi, M_{zz})/\partial(x, y)$, is familiar from many studies of passive scalar dispersion in quasi-geostrophic flows: in the present context the scalar is the complex field M_{zz}.

The role of the dispersive term, $iN^2\nabla^2 M/2f_0$, is isolated by taking $\beta = \Psi = N_z = 0$. Then plane wave solutions of (3.8), with $M \propto \exp(ikx + imz - i\omega t)$, have the dispersion relation

$$\omega = \frac{N^2k^2}{2f_0m^2}. \tag{3.9}$$

If the frequency in (3.9) is added to the 'carrier frequency,' f_0 in (3.1a), the result is the usual two term expansion of the internal wave dispersion relation around f_0.

The refractive term, $i[\beta y + (½)\nabla^2\Psi]M_{zz}$, is a spatially dependant correction of the local inertial frequency. The physics can be isolated by Kunze's (1985) WKB calculation which identifies the combination $f_0 + \beta y + (½)\nabla^2\Psi$ as an 'effective inertial frequency.' Because (3.8) is obtained without spatial scale separation assumptions, Kunze's result is more general than its WKB derivation suggests.

c. Special case: a vertically sheared current. Now suppose that $\Psi = V(z)x$ so that geostrophic velocity, $V = \Psi_x$, is vertically sheared and independent of the horizontal coordinates. For simplicity, also take $\beta = 0$. After these simplifications we are considering the propagation of NIOs through strongly sheared, unidirectional, geostrophic currents (e.g., Mooers, 1975a,b). One issue which turns out to be rather subtle here is the role of the vertical buoyancy gradient associated with the geostrophic flow. Notice that with $q = 0$ (the scaling used to obtain (3.2)) the term B_z in (2.11e) appears at leading order, along with the resting stratification, N^2. However, Mooers dropped this term from the outset. While this approximation is widely accepted, there is no justification for it if one takes $q = 0$ in the systematic expansion used in Section 2. We return to this issue below.

After the simplifications described above, (3.2a) reduces to

$$M_{zzt} + (VM_{yz})_z + \frac{i}{2}[\nabla\cdot(f_0^{-1}N^2 + V_{zz}x)\nabla M - (V_zM_x)_z - (V_zM_z)_x] = 0, \tag{3.10a, b}$$

$$M_{zzt} + (VM_{yz})_z + \frac{i}{2}(f_0^{-1}N^2 + V_{zz}x)\nabla^2 M - iV_zM_{xz} = 0.$$

The form in (3.10a) is obtained using the definition of the bracket in (3.2b). The equivalent form in (3.10b) is obtained using the alternative expression for the bracket in (3.4a). It is also easy to 'expand the differential operators' and verify directly that (3.10a) simplifies to (3.10b).

We emphasize the equivalence of (3.10a) and (3.10b) because a subtlety arises if one now makes an approximation by neglecting the vertical buoyancy gradient associated with the geostrophic flow, $f_0 V_{zz} x$, relative to the 'resting stratification', N^2. Dropping the term $V_{zz}x$ in (3.10a), and then expanding the differential operators, produces

$$M_{zzt} + (VM_{yz})_z + \frac{i}{2} f_0^{-1} N^2 \nabla^2 M - iV_z M_{xz} - \frac{i}{2} V_{zz} M_x = 0. \tag{3.11}$$

Because of the term $V_{zz}M_x$ the approximation (3.11) differs from the result of dropping the term $V_{zz}x$ in (3.10b). In other words, the order in which one performs the operations of approximation and expansion matters: the difference boils down to the final term $(i/2)V_{zz}M_x$ in (3.11). The answer in (3.11) is preferred because this approximation, in common with its exact ancestors in (3.10), conserves the energy, $M_z M_z^*$. (And, if one discards the term $V_{zz}x$ in (3.10b) then the resulting equation does not have an energy equation law.)

Comparing (3.10) with (3.8) we see that vertical shear results in two processes that do not appear in the barotropic case, (3.8). First, there is modification of the vertical buoyancy gradient by the geostrophic flow. It is clear physically that there must be such an effect, though we hope it will be unimportant, and the approximation in (3.11) can be used to enforce this prejudice.

The second new process in (3.10) and (3.11) is the 'cross-differentiated' term, $iV_z M_{xz}$. This term produces a qualitative change in the dispersion relation. The new process can be quickly isolated by limiting attention to shear flows with $V_{zz} = 0$ and NIOs with $M_y = 0$. Plane wave solutions, with $M \propto \exp\,[ikx + imz - i\omega t]$, then have the dispersion relation

$$\omega = \frac{N^2}{2f_0} \frac{k^2}{m^2} - V_z \frac{k}{m}. \tag{3.12}$$

Kunze (1996) noted that the modified NIO dispersion relation (3.12) implies that there is a frequency minimum

$$\omega_{\min} = f_0 \left[1 - \frac{V_z^2}{2N^2} \right], \tag{3.13}$$

at $k/m = f_0 V_z / N^2$. The physical interpretation of this result, given by Mooers (1975a,b) and Kunze (1996), is that NIOs with $k/m = f_0 V_z / N^2$ move particles in the plane of the sloping isopycnals.

4. Further simplifications contingent upon weaker vertical variation of the geostrophic background

To obtain the NIO equation (3.2) we assumed that the geostrophic flow had the same vertical scale as the NIOs: this was the choice $q = 0$ made in Section 2c. This scaling implies that the geostrophic background is strongly inhomogeneous in the z-direction. The strong vertical inhomogeneity leads to the complicated differential operators in (3.2). The different special cases considered in Section 3 show that this complexity is the price one pays for an approximation capturing all of the processes which occur as NIOs propagate through a three-dimensional geostrophic flow. However, typical oceanic currents have vertical shears which are weaker than those implied by the $q = 0$ scaling. We now investigate the simplifications which follow by taking $q = 2$ in (2.11).[4]

With $q = 2$, the vertical scale of Ψ in (3.1) is λ_V/ϵ^2 and all of the "geostrophic z-derivatives" in (2.11) are weakened by a factor of ϵ^2 relative to their former strength in Section 2d and e. As a result, many terms which previously appeared at leading order are now relegated to higher order. Thus, the resulting approximation contains fewer terms than the earlier expansion in Section 2. The reader might wonder why it is necessary to return to the primitive equations in (2.11)? Why not simplify (3.2) directly? Because the z-dependence of Ψ is weak, it is not obvious *a priori* how to pass the z-derivatives through coefficient functions involving Ψ in (3.2). For instance, the simplest approximation of (3.2) drops $O(\epsilon^2)$ terms, such as $\nabla\tilde{\Psi}_z$, and also pulls all z derivatives through the brackets so that only M is differentiated with respect to z. Thus, for example, one would use the following simplification:

$$i[(\beta y + \tfrac{1}{2}\nabla^2\Psi)M_z]_z = i(\beta y + \tfrac{1}{2}\nabla^2\Psi)M_{zz} + O(\epsilon^2). \tag{4.1}$$

This approximation of (3.2) amounts to treating the z dependence of Ψ as parametric so that the result is identical to the barotropic special case in (3.8). However, if $\Psi_z \neq 0$, then (3.8) does not conserve energy. We now show that a systematic expansion, starting with $q = 2$ in (2.11), results in a simplified version of (3.2) that does have an energy conservation law.

a. An expansion with weaker vertical variation of the geostrophic flow. We now summarize the results of applying the ϵ^2 expansion to (2.11). In terms of dimensional variables, the leading order fields are

$$\begin{aligned} u_0 + iv_0 &= e^{-if_0t}M_z, \\ w_0 &= -M_\xi e^{-if_0t} + \text{c.c.} \\ b_0 &= i\frac{N^2}{f_0}M_\xi e^{-if_0t} + \text{c.c.} \end{aligned} \tag{4.2a–c}$$

The expressions above are the dimensional analogs of those in (2.17), (2.18) and (2.20), except that b_0 is now simplified.

The leading order pressure can be calculated explicitly if one introduces a complex field $A(x, y, z, t)$ defined by

$$(f_0^2/N^2)A_z \equiv M. \tag{4.3}$$

4. We jump from $q = 0$ to $q = 2$ because the choice $q = 1$ produces both odd and even powers of ϵ in (2.11): this forces an expansion in all powers of ϵ. Following this route, at $O(\epsilon^2)$, one obtains the result (4.5), otherwise obtained by taking $q = 2$ and expanding only in powers of ϵ^2. Thus, mainly for ease of exposition, we prefer to take $q = 2$ so that only even powers of ϵ appear in (2.11).

In terms of A, the pressure is

$$p_0 = if_0 A_\xi e^{-if_0 t} + \text{c.c.} \tag{4.4}$$

We defer determination of the constant of integration in (4.4) to the discussion surrounding Eqs. (4.8) and (4.9).

The evolution equation is obtained by setting all terms involving $\exp(-if_0 t)$ in R_0 equal to zero. At this point, there is a difference between the present expansion and the earlier procedure in Section 2: there we did not have a convenient expression for p_0 and so instead we eliminated the resonant terms in R_{0z}. Now, with (4.4), we can avoid this detour and perform the elimination directly in R_0. The result is most naturally written as an equation for A:

$$LA_t + \frac{\partial(\Psi, LA)}{\partial(x, y)} + \frac{i}{2} f_0 \nabla^2 A + i\left(\beta y + \frac{1}{2}\nabla^2\Psi\right) LA = 0, \tag{4.5}$$

where L is the differential operator defined by

$$LA \equiv (f_0^2 N^{-2} A_z)_z. \tag{4.6}$$

The M-equation in (3.2) is obtained by noting that $M_z = LA$, and then taking the z-derivative of (4.5). The result is

$$M_{zzt} + \left[\frac{\partial(\Psi, M_z)}{\partial(x, y)}\right]_z + \frac{i}{2}\frac{N^2}{f_0}\nabla^2 M + i\left[\left(\beta y + \frac{1}{2}\nabla^2\Psi\right) M_z\right]_z = 0. \tag{4.7}$$

Eq. (4.7) is a simplified version of (3.2): various "cross terms" involving $\nabla\Psi_z$ are gone, and $(N^2/f_0) + \Psi_{zz}$ has been replaced by N^2/f_0. Eq. (4.7) conserves the NIO energy, $M_z M_z^*/2$.

Eqs. (4.5) and (4.7) are equivalent and, in applications, it might be better to work with (4.5) because the advective term is more intuitive, and because the leading order pressure in (4.4) is directly related to A. The formulation in terms of A also has the advantage that the first term in (4.5) has an immediate physical interpretation viz., since $u_0 + iv_0 = e^{-if_0 t} LA$, LA_t is the rate of change of the demodulated velocity.

van Meurs (1997) has recently obtained an approximation equivalent to (4.5). van Meurs writes his equation using an integral operator denoted by I. The connection between (4.5) and the formulation of van Meurs is made by noting that I is the inverse of the differential operator L.

We now turn to the issue of determining the constant of integration in the definition, (4.4), of A. First, observe that the boundary conditions on A are

$$A_z(x, y, 0, t) = A_z(x, y, -H, t) = 0. \tag{4.8}$$

The conditions above ensure that w_0 in (4.2b) is zero at the top and bottom of the ocean, and that the barotropic mode is eliminated. Vertically integrating (4.5) over the depth of the ocean, one obtains

$$\frac{i}{2} f_0 \nabla^2 \int_{-H}^{0} A \, dz = 0. \tag{4.9}$$

The "consistency condition" in (4.9) is satisfied by choosing the constant of integration in (4.4) so that the vertical integral of A is zero. This choice ensures that the vertically integrated NIO pressure is also zero: once again, this is the elimination of the barotropic mode.

To summarize, with weak geostrophic stratification, $q = 2$, there are two equivalent formulations: the A-equation in (4.5) and its derivative, the M-equation in (4.7). In the strong stratification limit, $q = 0$, we have only the M-equation in (3.2). In this case, there is no equivalent A-equation because terms such as $\nabla \cdot (\nabla \tilde{\Psi}_z M_z)$ prevent one from integrating (3.2) in z.

b. A comparison of the approximations with the exact system. To develop more confidence in the various NIO approximations it is useful to make comparisons between solutions of the approximate equations and those of the full equations of motion. A relatively simple, but nontrivial, case is obtained by considering a vertically sheared, steady geostrophic flow given by

$$\Psi = -syz. \tag{4.10}$$

The geostrophic velocity is $(U, V, W) = (sz, 0, 0)$ and the geostrophic buoyancy is $B = -sf_0 y$. Let us compare the predictions of our two approximations, (3.2) and (4.7), with an exact solution of (2.3). To isolate the effects of the vertical shear we take $\beta = 0$.

We begin with the exact solution: define a tilting wavenumber

$$m(t) = m_0 - kst, \tag{4.11}$$

so that the instantaneous intrinsic wave frequency is

$$\hat{\omega}(t) \equiv \sqrt{f_0^2 + N^2 \frac{k^2 + l^2}{m^2}}. \tag{4.12}$$

If m_0, k and s are all positive then $m(t)$ in (4.11) is decreasing. In this case, the steady geostrophic shear flow, $U = sz$, is systematically increasing the frequency of a plane wave. Thus, a wave which is an NIO at $t = 0$ is being shifted away from the near inertial part of the spectrum. Consequently, the approximations of Sections 2 and 3 must ultimately fail: this breakdown is certainly before the finite time at which $m = 0$. In the following discussion we assess the limits of validity of the approximations by studying this secular failure.

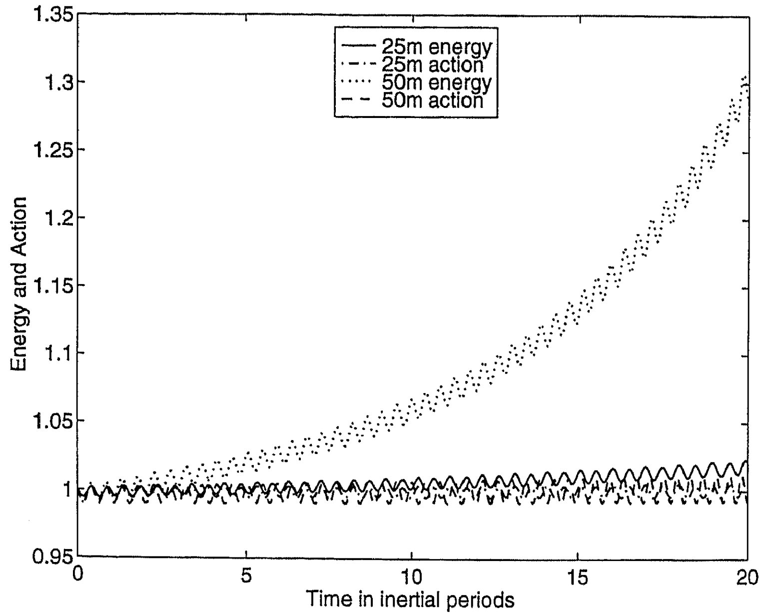

Figure 1. Energy and action obtained by numerically integrating (4.14) with $k = l = 2\pi/20$ km, $f_0 = 10^{-4}$ s^{-1}, $s = 2f_0$ and $N = 100 f_0$. With both $m_0 = 2\pi/50$ m and $m_0 = 2\pi/25$ m the action is more nearly constant than the energy.

Using $m(t)$, one can write a plane wave solution of (2.3) as

$$[u, v, w, p, b] = [\hat{u}(t), \hat{v}(t), \hat{w}(t), \hat{p}(t), \hat{b}(t)]e^{ikx+ily+imz}. \tag{4.13}$$

Putting (4.13) into (2.3), and eliminating $\hat{p}$ and $\hat{w}$, leads to the system

$$\frac{d}{dt}\begin{pmatrix}\hat{u}\\ \hat{v}\\ \hat{b}\end{pmatrix} = \begin{bmatrix} sk/m & f_0 + (sl/m) & -k/m \\ -f_0 & 0 & -l/m \\ N^2k/m & sf_0 + (N^2l/m) & 0 \end{bmatrix}\begin{pmatrix}\hat{u}\\ \hat{v}\\ \hat{b}\end{pmatrix}. \tag{4.14}$$

A numerical integration of (4.14) is summarized in Figure 1 by showing the energy and action densities as a function of time. The energy density of the internal wave

$$\hat{E} \equiv \tfrac{1}{2}[\hat{u}^2 + \hat{v}^2 + N^{-2}\hat{b}^2], \tag{4.15}$$

is not conserved. However, the action density

$$\hat{A} \equiv \frac{\hat{E}}{\hat{\omega}}, \tag{4.16}$$

exhibits much smaller changes than $\hat{E}$ (Bretherton and Garrett, 1968). In Figure 1, the wave which has an initial vertical wavelength of 25 m remains nearly inertial; this wave has negligible changes in both action and energy. However, the second wave, with an initial vertical wavelength of 50 m, is shifted out of the near-inertial part of the spectrum. This second wave exhibits a significant increase in its energy density.

The two approximations, (3.2) and (4.7), can be solved analytically by writing

$$M = \frac{P(t)}{m^2(t)} e^{ikx+ily+imz}. \tag{4.17}$$

Putting (4.17) into (3.2) and (4.7) gives

$$\begin{aligned} \frac{dP_3}{dt} &= -i\left(\frac{N^2}{2f_0}\frac{k^2+l^2}{m^2} + s\frac{l}{m}\right)P_3 - s\frac{k}{m}P_3, \\ \frac{dP_4}{dt} &= -i\left(\frac{N^2}{2f_0}\frac{k^2+l^2}{m^2}\right)P_4 - s\frac{k}{m}P_4, \end{aligned} \qquad (4.18\text{a, b})$$

where P_3 is the result from (3.2) and P_4 that of (4.7).

From (4.18) it follows that

$$E = M_z M_z^* = \frac{|P_n|^2}{m^2}, \tag{4.19}$$

($n = 3$ and 4) is constant: both approximations predict that the energy density is constant. The first comparison we can make is between (4.19) and the results in Figure 1. Clearly, after 20 inertial periods, the approximation has failed for the wave which began with a vertical wavelength of 50 m. However, the calculation in Figure 1 uses a choice of parameters that is hostile to the assumptions of the approximation. For instance, the vertical shear is $s = 2 \times 10^{-4}\ \mathrm{s}^{-1}$, which is equivalent to a velocity difference of 20 cm s^{-1} over 100 m. The ratio N/f_0 is 100. Reducing either of these numbers will prolong the near inertial stage of the wave evolution and result in smaller changes in energy over 20 inertial periods.

The conservation law in (4.19) suggests the introduction a phase variable, $\phi_n(t)$, defined by

$$P_n = m\sqrt{E}e^{i\phi_n}. \tag{4.20}$$

Using (4.20) in (4.18) one has

$$\begin{aligned} \frac{d\phi_3}{dt} &= -\frac{N^2}{2f_0}\frac{k^2+l^2}{m^2} - s\frac{l}{m}, \\ \frac{d\phi_4}{dt} &= -\frac{N^2}{2f_0}\frac{k^2+l^2}{m^2}. \end{aligned} \qquad (4.21\text{a, b})$$

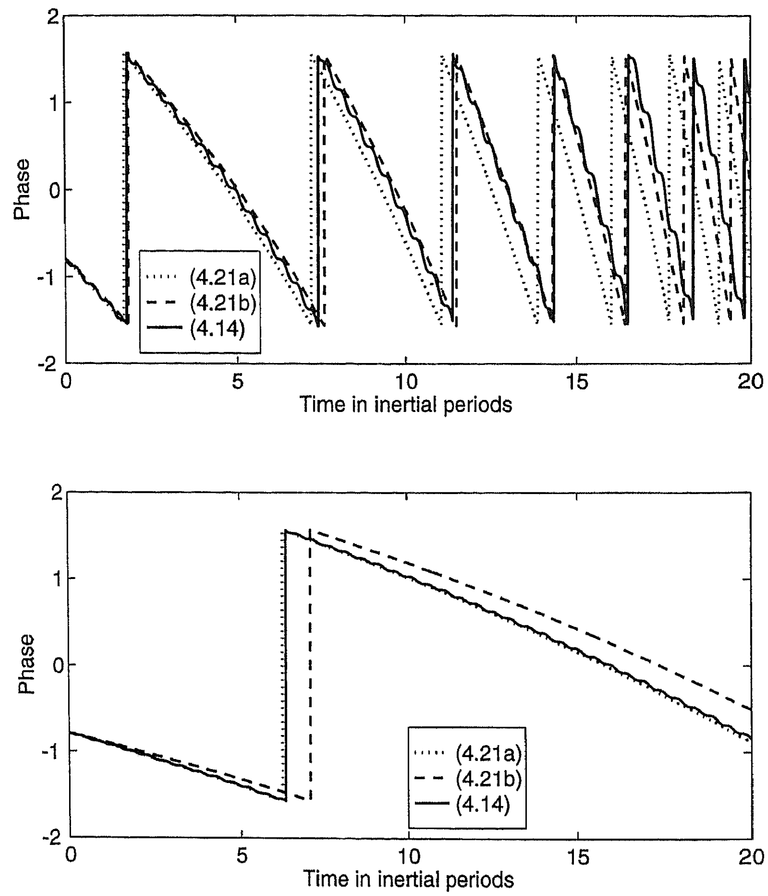

Figure 2. The phase of the demodulated velocity, $\exp(if_0t)(u + iv)$, as a function of time. The parameters are $k = l = 2\pi/20$ km, $f_0 = 10^{-4}$ s^{-1}, $s = 2f_0$ and $N = 100f_0$. In the top panel $m_0 = 2\pi/50$ m, while in the bottom panel $m_0 = 2\pi/25$ m. The phase jumps discontinuously between $\pi/2$ and $-\pi/2$ because of the definition of arctangent we employ.

Performing the quadratures in (4.21) we obtain

$$\phi_3 = \phi(0) + \frac{N^2}{2f_0}\frac{k^2 + l^2}{sk}\left[\frac{1}{m_0} - \frac{1}{m}\right] + \frac{l}{k}\ln\left|\frac{m}{m_0}\right|,$$

$$\phi_4 = \phi(0) + \frac{N^2}{2f_0}\frac{k^2 + l^2}{sk}\left[\frac{1}{m_0} - \frac{1}{m}\right]. \qquad (4.22\text{a, b})$$

These results show that the two approximations differ only in their handling of the phase evolution of the NIOs: the more complicated approximation (3.2) introduces the logarithmic correction in (4.22a).

Figure 2 compares (4.22) with the results of a numerical integration of (4.14). The top panel shows the phase of the demodulated velocity [i.e., the phase of exp $(if_0t)(u + iv)$] as a function of time when $m_0 = 2\pi/50$ m and the bottom panel show the case in which $m_0 = 2\pi/25$ m. The comparison is interesting because in the top panel ϕ_4 is more accurate than ϕ_3, while in the bottom panel the reverse is the case!

Why is the simple approximation (4.7) sometimes more accurate than the more elaborate approximation (3.2)? The answer is that both of these approximations are probably asymptotic (rather than convergent). Asymptotic expansions have the property that adding additional terms does not always improve accuracy. The results in Figure 2 (and others we have obtained) support this interpretation. Suppose that the initial parameters k, l, N, s and f_0 are fixed and only m_0 varies. Then, when m_0 is large enough (i.e., when $\epsilon \propto \lambda_V \propto m_0^{-1}$ is small enough), ϕ_3 is a better approximation than ϕ_4. But there is also a range of moderately small ϵ in which ϕ_4 is superior to ϕ_3 (e.g. the top panel of Fig. 2).

5. Propagation of NIOs through a geostrophic flow with smaller horizontal scale

a. Observational motivation. We now turn to an application of the NIO equation (3.2). In this section, we propose an explanation for observations made by D'Asaro *et al.* (1995) in the northeast Pacific Ocean during the Ocean Storms Experiment. These authors observed that a strong October storm generated NIOs in the mixed layer with a horizontal scale that greatly exceeded the Rossby radius of deformation. Because NIOs have both large horizontal scale and small vertical scale, linear theory predicts that they propagate extremely slowly. However, the observations show that 21 days after the storm the inertial energy in the mixed layer has been reduced to background levels. The formation of an inertial "beam" below the mixed layer strongly suggests that this reduction occurs because of inexplicably rapid vertical propagation of NIO energy.

One possible explanation of the rapid radiation of NIO energy is D'Asaro's (1989) result that the β-effect can accelerate the propagation of NIOs by decreasing the horizontal scale of the wave field [$l(t) = l(0) - \beta t$ where $l(t)$ is the meridional wavenumber of the NIOs]. This decrease in horizontal wavelength was observed by D'Asaro *et al.* and is sufficient to explain the southward propagation of the lowest vertical modes. However, the observed decrease in mixed layer inertial energy and shear to background levels in 21 days is still significantly faster than estimates based on linear NIO propagation in an ocean whose only inhomogeneity is the β-effect. The problem is particularly acute for the shear, which is contained mostly in the higher vertical modes; according to the internal wave dispersion relation, near inertial shear should remain in the mixed layer for months, even with the β-shift.

These negative conclusions were reinforced in two subsequent papers. D'Asaro (1995a) simulated NIO propagation using a two-dimensional nonlinear model with realistic wind-forcing and stratification. The model failed to rationalize the observations because (a) the observed NIO energy in the mixed layer decayed much more rapidly than the model NIO energy (b) the observed shear at the base of the mixed layer decayed much more rapidly than the model shear.

D'Asaro (1995b) examined the effect of mesoscale currents (i.e., the geostrophic flow, Ψ) on NIOs. The main theoretical result used by D'Asaro (1995b) to interpret the observations is Kunze's (1985) conclusion that the geostrophic flow produces an effective inertial frequency

$$f_{\text{eff}} = f_0 + \beta y + \tfrac{1}{2}\nabla^2\Psi. \tag{5.1}$$

Kunze (1985) used the WKB approximation to identify the important combination in (5.1). But without the WKB approximation, the same pattern, $\beta y + \nabla^2\Psi/2$, appears in (3.2) and, more transparently, in (4.5). The WKB interpretation of (5.1) is that the frequency of NIOs should be shifted by $\nabla^2\Psi/2$. However, D'Asaro (1995b) concluded that the observed frequency shifts were smaller by at least a factor of five than $\nabla^2\Psi/2$. But, since the NIO fields have much larger spatial structure than the mesoscale eddies, the WKB approximation is invalid and interpretation of (5.1) as implying a simple shift in frequency requires reassessment. This reassessment, together with an explanation of the rapid decay of mixed layer NIO shear, is the goal of this section.

b. The scale separation assumption. Motivated by the observations summarized above, we will now use the NIO equation to examine the limit in which the geostrophic currents have much smaller horizontal scale than the NIO. The small parameter is

$$\begin{aligned} \mu &\equiv \frac{\text{length scale of geostrophic eddies}}{\text{length scale of NIO's}}, \\ &= \frac{l}{\lambda_H}. \end{aligned} \tag{5.2a, b}$$

The WKB approximation assumes that μ is large, so that the medium is locally homogeneous, and ray tracing concepts, such as 'local wavenumber' and 'group velocity,' are sensible. Here instead, with $\mu \ll 1$, the NIOs propagate through a rapidly varying medium whose wave-scale properties result from an average over the small scale geostrophic turbulence.

Because the familiar concepts of group velocity and local wavenumber are useless in this problem, some readers may find it instructive to consider an alternative oceanographic problem in which a scale separation approximation analogous to $\mu \ll 1$ is made. This is the dispersion of a passive scalar by geostophic turbulence. The passive scalar, concentration $\theta(x, y, t)$, satisfies an advection diffusion equation

$$\theta_t + \frac{\partial(\Psi, \theta)}{\partial(x, y)} = \kappa\nabla^2\theta, \tag{5.3}$$

where Ψ is the geostrophic stream function and κ is the submesoscale diffusivity. On length scales larger than those of the geostrophic stream function, the spatially averaged tracer concentration, $\overline{\theta}$, satisfies

$$\overline{\theta}_t = \kappa_e \nabla^2 \overline{\theta}, \tag{5.4}$$

where κ_e is the eddy diffusivity.[5] A systematic derivation of the mean field equation (5.4) uses the scale separation in (5.2) to justify κ_e as a closure of the $\overline{\mathbf{u}'\theta'}$ correlation that appears when one spatially averages (5.3) (e.g., Moffatt, 1983; Rhines, 1986).

In the following section we will apply analogous averaging arguments to the NIO equation (4.5). One can consider A to be a passive, complex scalar, just as θ is a passive, real scalar. One can define a mean field, $\overline{A}$, just as one defines $\overline{\theta}$. The issue is, how does averaging over small-scale geostrophic eddies effect the dynamics of the passive complex scalar A? What is the mean field description, analogous to (5.4), of $\overline{A}$?

c. *Heuristic averaging arguments.* Appendix B addresses the problems posed at the end of the previous section using a multiple length-scale expansion. However, there are relatively simple heuristic arguments that help one understand the result of this calculation in physical terms. Suppose that the small-scale geostrophic eddies are barotropic, so that we can use the A-equation in (4.5). We also take $\beta = 0$ and assume that the eddies are steady, $\Psi_t = 0$. Then integrating (4.5) over a large horizontal area we obtain

$$\partial_t \iint LA\, dxdy + \frac{i}{2} \iint \nabla^2 \Psi LA\, dxdy = 0, \tag{5.5}$$

where LA is defined in (4.6). If $\nabla^2\Psi = 0$ then, from (5.5), we obtain the well-known result that the zero horizontal wavenumber component of an NIO does not propagate vertically. That is to say, the quantity $\iint LA\, dxdy$ (which is a function of z) remains equal to its initial value.

Now suppose that the initial condition is a pure inertial oscillation, with no horizontal gradients. Horizontal inhomogeneities in the environment (e.g. $\nabla^2\Psi \neq 0$) will then create inhomogeneities in the NIO so that the second term in (5.5) becomes nonzero. *If* systematic correlations develop between A and $\nabla^2\Psi/2$ then there will be secular changes in the large scale field. We now show there is a potent mechanism for inducing these $A - \nabla^2\Psi$ correlations.

Begin by partitioning A according to

$$A(x, y, z, t) = \overline{A}(z, t) + A'(x, y, z, t), \tag{5.6}$$

where $\overline{A}(z, t)$ is the horizontal average of A, and A' is the remainder or fluctuation. Putting (5.6) into (5.5) we have

$$L\overline{A}_t + \frac{i}{2}\overline{\nabla^2\Psi LA'} = 0. \tag{5.7}$$

5. Strictly speaking, there is an eddy diffusivity tensor, and also advection by mean flow. For expository purposes we confine attention to the simplest case of homogeneous, isotropic eddies with no mean flow.

The term $\overline{\nabla^2\Psi LA'}$ is analogous to $\overline{\mathbf{u}'\theta'}$ in the eddy-diffusion problem: our goal is to close (5.7) by expressing $\overline{\nabla^2\Psi LA'}$ in terms of $\overline{A}$.

Subtracting (5.7) from the full A-equation in (4.5) we obtain the fluctuation equation:

$$LA'_t + \frac{\partial(\Psi, LA')}{\partial(x, y)} + \frac{i}{2}f_0\nabla^2 A' + \frac{i}{2}\nabla^2\Psi LA' - \frac{i}{2}\overline{\nabla^2\Psi LA'} = -\frac{i}{2}\nabla^2\Psi L\overline{A}. \quad (5.8)$$

The term on the right-hand side of (5.8) is a source term for A': if one considers an initial condition in which $A' = 0$, then the right-hand side of (5.8) is the mechanism through which A' is produced by the small-scale geostrophic vorticity interacting with the mean field, $\overline{A}$.

Eq. (5.8) can be viewed as a linear equation for A', forced by $\nabla^2\Psi L\overline{A}$. If we could solve this equation for A' in terms of $\nabla^2\Psi L\overline{A}$, then the result could be substituted into (5.7) to obtain a closed equation for $\overline{A}$. This strategy is too ambitious because (5.8) is too difficult to treat exactly. However, in the limit where Ψ is weak enough (more details are given below in Section 5d), there is a simple dominant balance in (5.8) between the horizontal dispersive term, $(if_0/2)\nabla^2 A'$ and the production term on the right-hand side. This dominant balance, $f_0\nabla^2 A' \approx -\nabla^2\Psi L\overline{A}$, implies that the approximate solution of (5.8) (obtained by 'cancelling the Laplacians') is

$$A' \approx -\frac{1}{f_0}\Psi L\overline{A}. \quad (5.9)$$

Eq. (5.9) is the 'strong dispersion approximation': the terminology is explained below in Section 5d.

Putting (5.9) into (5.7) one has

$$L\overline{A}_t + \frac{i}{2f_0}\overline{\nabla\Psi\cdot\nabla\Psi}L^2\overline{A} = 0. \quad (5.10)$$

Eq. (5.10) is a *vertical* wave propagation equation (essentially, a Schrödinger equation) for the quantity $L\overline{A}$.

Notice that $\overline{A}(z, t)$ has no structure on the eddy scale. However, the fluctuation, A' in (5.9), is directly proportional to the eddy stream function, Ψ. The averaged eddy kinetic energy, $\overline{\nabla\Psi\cdot\nabla\Psi}$, appears as a coefficient in (5.10) because of the identity $\overline{\Psi\nabla^2\Psi} = -\overline{\nabla\Psi\cdot\nabla\Psi}$. It is an interesting prediction of this calculation that it is the eddy stream function Ψ, and not the eddy vorticity, $\nabla^2\Psi$, which contains the small-scale structure of the NIO. Although it is the eddy vorticity on the right hand side of (5.8) that forces A', the Laplacian is 'cancelled' when this term is balanced by NIO wave dispersion, $(if_0/2)\nabla^2 A'$.

Earlier studies, using specific models for the geostrophic flow, Ψ, have emphasized that NIO activity is concentrated within regions of negative $\nabla^2\Psi$ (Kunze, 1985; Rubenstein and Roberts, 1986; Klein and Treguier, 1995). At first glance, it seems difficult to reconcile (5.9) with these earlier conclusions. However, there is a direct connection, as one can see by considering an example:

$$\Psi = \Psi_0 \cos(py). \tag{5.11}$$

Suppose also that N is constant, and that the mean field is the n'th vertical mode i.e., $\overline{A} = \cos(n\pi z/H)$. (There is no loss of generality here: linear superposition can be used to construct an arbitrary $\overline{A}$.) Using (5.9), the total NIO field is:

$$\overline{A} + A' = \left[1 + \frac{\Psi_0}{f_0 R_n^2}\cos py\right]\cos(n\pi z/H), \tag{5.12}$$

where $R_n \equiv NH/n\pi f_0$ is the deformation radius of the n'th vertical mode. Eq. (5.12) shows how the total NIO field is modulated on the eddy length-scale, p^{-1}, and that the largest amplitude is in the regions in which $\cos py$ is close to 1. Since $\nabla^2\Psi = -p^2\Psi_0 \cos py$, the maxima of A coincide with the negative vorticity regions.

The argument above is not limited to the specific example in (5.11): Ψ is negatively correlated with $\nabla^2\Psi$, and $-L$ is a positive definite differential operator. Thus A' in (5.9) adds constructively to $\overline{A}$ in regions of negative vorticity.

d. Discussion of the strong dispersion approximation, (5.9). We now return to the approximations involved in obtaining (5.9) as the solution of (5.8). Notice A' in (5.8) is linearly proportional to Ψ. Thus, *a posteriori,* all of the neglected terms, such as $\partial(\Psi, A')/\partial(x, y)$, are $O(\Psi^2)$.[6] If Ψ is 'small enough' then these $O(\Psi^2)$ terms will be less than the two $O(\Psi)$ terms which have been retained in (5.9).

'Small enough' means that the horizontal wave dispersion, $(i/2f_0)\nabla^2 A$, is strong enough to prevent large distortions of the mean field i.e., $\overline{A} \gg A'$. In the specific example (5.12), this means that

$$\Upsilon_n \equiv \frac{\Psi_0}{f_0 R_n^2} \tag{5.13}$$

should be small to ensure the validity of (5.9). The condition $\Upsilon_n \ll 1$ is also obtained by evaluating the ratio of the neglected term, $\nabla^2\Psi L A'$, to the retained term $f_0\nabla^2 A'$ in (5.8). Using $L \sim (f_0/N\lambda_V)^2$ one has

$$\frac{\nabla^2\Psi L A'}{f_0 \nabla^2 A'} \sim \frac{\Psi f_0}{N^2\lambda_V^2}. \tag{5.14}$$

(Because Ψ and A' vary on the same horizontal length scale, ∇^2 cancels in the estimate above.) Using $N\lambda_V/f_0 R_n \sim 1$ we see that (5.14) is equivalent to (5.13). (Here λ_V is the vertical length scale of the n'th vertical mode.)

6. An apparent exception is the term LA_t' in (5.8). But from (5.10) we see that $L\overline{A}_t$ is $O(\Psi^2)$ so then, using (5.9), LA_t' is $O(\Psi^3)$.

The crucial point is that $R_n \rightarrow 0$, and $\Upsilon_n \rightarrow \infty$, as n becomes large. Thus, the strong dispersion approximation, (5.9), is not valid for high vertical modes. Physically, higher vertical modes have weaker horizontal dispersion. In terms of the example in (5.12), if n is too large the term $(\Psi_0/f_0R_n^2) \cos py$ is $O(1)$ (or large) and the NIO develops large modulations on the eddy scale, p^{-1}. This signals the failure of approximation (5.9).

Now let us evaluate the nondimensional number in (5.13) using the Ocean Storms region as an example. From D'Asaro *et al.* (1995), the RMS eddy velocity is about 5 cm s^{-1} and the eddy length scale is 40 km. Using the model in (5.11), $p = 2.5 \times 10^{-5}$ m^{-1} and $\Psi_0 = 2.83 \times 10^3$ m^2 s^{-1}. The maximum vorticity gradient is $p^3\Psi_0 = 4.42 \times 10^{-11}$ m^{-1} s^{-1}, or roughly four times the β-effect.

Table 1 of D'Asaro *et al.* provides the modal phase speeds, $c_n = f_0R_n$, for the Ocean Storms region. Using $f_0 = 1.07 \times 10^{-4}$ s^{-1} we find $R_1 = 21.3$ km and:

$$\Upsilon_1 \approx 0.06 \ll 1. \tag{5.15}$$

We conclude that the strong dispersion approximation is valid for the first mode. But for mode number 5, $R_5 = 4.8$ km and then:

$$\Upsilon_5 \approx 0.86 \tag{5.16}$$

Thus, for the Ocean Storms region, the small Υ assumption starts to fail at around vertical mode number 5.

e. Radiation of NIOs from the mixed layer. The heuristic arguments of the previous section, and the multiple scale analysis of Appendix B, result in the following mean field equation for NIOs with very large horizontal scale:

$$L\overline{A}_t + i\beta yL\overline{A} + \frac{i}{2}f_0\nabla^2\overline{A} + if_0^{-1}KL^2\overline{A} = 0. \tag{5.17}$$

In (5.17), $K \equiv \overline{\nabla\Psi \cdot \nabla\Psi}/2$ is the average kinetic energy of the small-scale geostrophic turbulence: the term containing K results from a closure of the $A' - \nabla^2\Psi$ correlation discussed in the previous sections. The other terms in (5.17) are well known processes, such as horizontal dispersion and the frequency shift due to β: see Appendix B.

In this subsection we discuss the effect of the new term, $if_0^{-1}KL^2A$, on the propagation of an initially compact NIO disturbance. We use the vertical normal mode approach of Pollard (1970) and Gill (1984), and for simplicity we take $\beta = 0$. In Gill's (1984) notation, the Sturm-Liouville problem associated with the linear operator L is

$$L\hat{p}_n + f_0^2c_n^{-2}\hat{p}_n = 0, \tag{5.18}$$

where the eigenvalue, c_n, is the speed of mode n. The solution of (5.17) can be represented as

$$\overline{A}(x, y, z, t) = \sum_{n=1}^{n=\infty} A_n(x, y, t)\hat{p}_n(z), \tag{5.19}$$

where the evolution equation for mode n is

$$A_{nt} - \frac{i}{2} R_n^2 f_0 \nabla^2 A_n - \frac{iK}{f_0 R_n^2} A_n = 0. \tag{5.20}$$

In (5.20), $R_n = c_n/f_0$ is the radius of deformation of mode n.

The dispersion relation is obtained by substituting $A_n = \exp(ikx + ily - i\omega_n t)$ into (5.20). The result is

$$\omega_n = \frac{1}{2} R_n^2 f_0 (k^2 + l^2) - \frac{K}{f_0 R_n^2}. \tag{5.21}$$

As $n \rightarrow \infty$, $R_n \rightarrow 0$. Thus, if $K = 0$, then $\omega_n \rightarrow 0$ as $n \rightarrow \infty$. This means that the high vertical modes all have the same frequency, f_0, and remain in phase for a long time. Consequently, a compact initial disturbance does not disperse. However, if $K \neq 0$, then the effect of the final term in (5.21) is to *increase* the frequency difference between high vertical modes. We show below that the ensuing rapid loss of phase coherence is responsible for a dramatic change in the dispersive properties of NIOs. It is remarkable that this effect is independent of the horizontal scale of the NIOs i.e., the final term in (5.21) is independent of (k, l).

In the discussion surrounding (5.15) and (5.16) we emphasized that the strong dispersion approximation is invalid for high vertical modes. This means that the dispersion relation (5.21) is not valid if n is large (and for 5 cm s^{-1} eddy-velocities we anticipate substantial errors when n is only 4 or 5). An improved calculation of A' from (5.8), avoiding the strong dispersion approximation in (5.9), would be of great interest. The following results, based on (5.21), should be regarded as suggestive, rather than conclusive.

Suppose that N is constant, so that the solution of (5.18) is

$$\hat{p}_n = \cos\left(\frac{n\pi z}{H}\right), \qquad c_n = \frac{NH}{n\pi}. \tag{5.22}$$

As an initial condition, suppose that

$$LA = e^{-z^2/2\delta^2} \cos ly. \tag{5.23}$$

Thus, at $t = 0$, $u = \cos ly \exp(-z^2/2\delta^2)$ and $v = 0$. The shear, u_z, is a maximum at $z = -\delta$.

With the initial condition in (5.23), the solution of (5.17) is that

$$LA = \cos ly \sqrt{2\pi} \frac{\delta}{H} \sum_{n=1}^{n=N} \exp\left[-\frac{1}{2}\left(\frac{\delta\pi}{H}\right)^2 n^2 - i\omega_n t\right] \cos\left(\frac{n\pi z}{H}\right). \tag{5.24}$$

To obtain (5.24), the integrals involved in the modal projection have been evaluated approximately using $\delta/H \ll 1$. The calculations reported below used $N = 400$ in (5.24).

Figures 3 and 4 shows the solution (5.24) using the parameter values

$$\delta = 50 \text{ m}, \qquad H = 5000 \text{ m}, \qquad f_0 = 10^{-4}\text{s}^{-1}, \qquad l = \frac{1}{600 \text{ km}}. \tag{5.25}$$

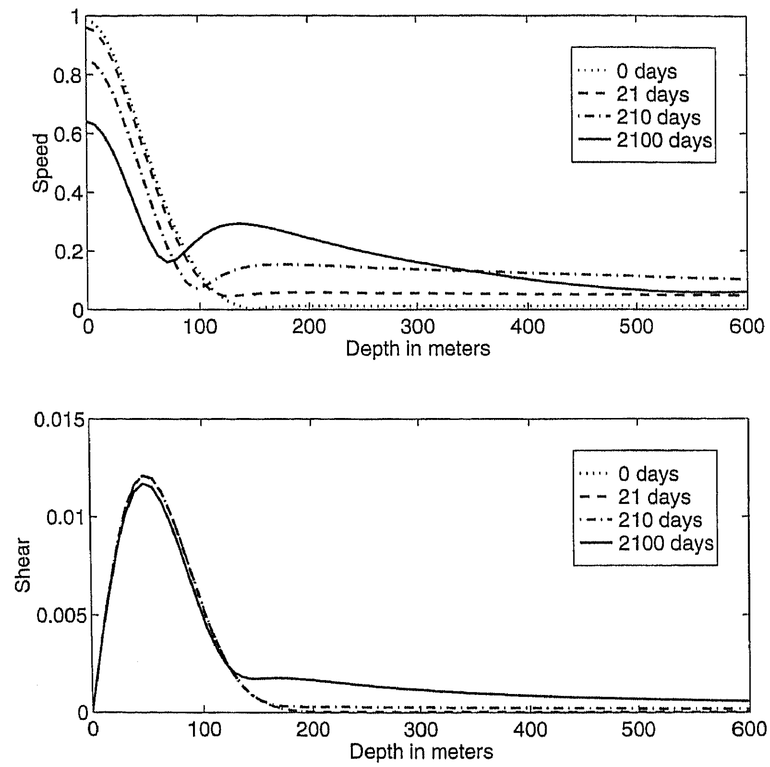

Figure 3. The speed, $\sqrt{u^2 + v^2}$ (upper panel) and the shear $\sqrt{u_z^2 + v_z^2}$ (lower panel) calculated from the solution in (5.24) using the numbers in (5.25), $N = 50f_0$ and $K = 0$. In this case, without a geostrophic flow, the vertical radiation of the NIOs is very slow.

Suppose that we take $N = 50f_0 = 5 \times 10^{-3}\ \mathrm{s}^{-1}$, which is a rather small value of N for the upper ocean. This choice implies that

$$R_n = \frac{NH}{\pi f_0}\frac{1}{n}, \qquad \approx \frac{80\ \mathrm{km}}{n}. \tag{5.26a, b}$$

The radius of deformation of the $n = 1$ mode in (5.34b) is unrealistically large. Our choice $N = 50f_0$ is a compromise between having a realistically strong buoyancy frequency in the upper ocean, and a realistically small first deformation radius.

In Figure 3, $K = 0$. Virtually nothing happens during the first 21 days. Even after about six years the shear is almost unchanged. The evolution is far too slow to explain the observations of D'Asaro *et al.* (1995). The choice of $N = 50f_0$ is not responsible for these problems: increasing N by a factor of $\sqrt{10}$, so that $N \approx 160f$ (unrealistically large), means

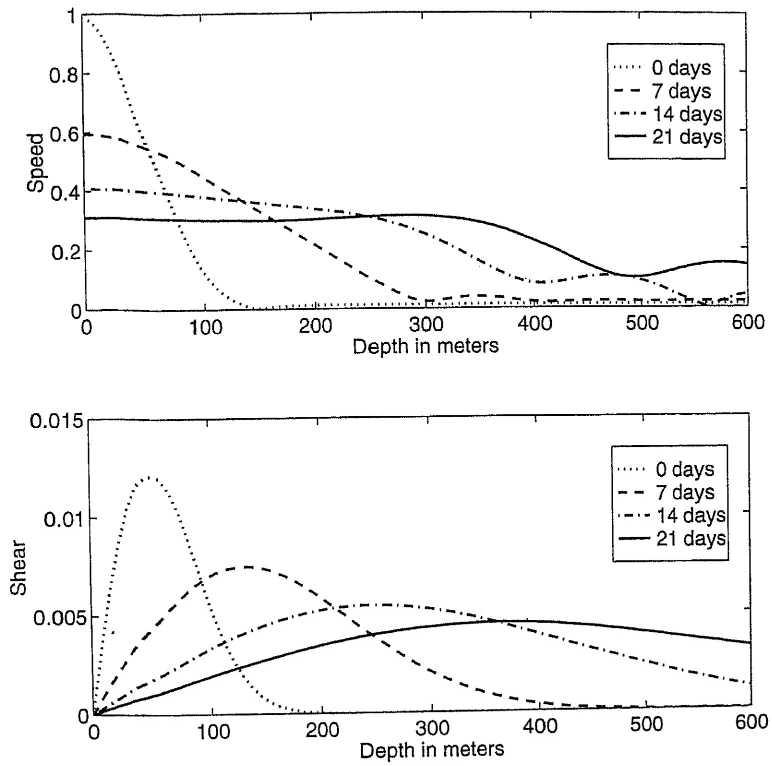

Figure 4. The speed, $\sqrt{u^2 + v^2}$ (upper panel) and the shear $\sqrt{u_z^2 + v_z^2}$ (lower panel) calculated from the solution in (5.24) using the numbers in (5.25), $N = 50f_0$ and $K = (1/800)\text{m}^2\,\text{s}^{-2}$. Notice that the level of maximum shear, initially at $z = -50$ m, now moves downwards much more rapidly than in Figure 3.

that curve labelled day 210 in Figure 3 now corresponds to day 21. The evolution is still orders of magnitude too slow. Even increasing l in (5.25) by a factor of 10 does not help: the shear in the lower panel of Figure 3 remains localized at its initial level. In particular, the shear maximum at $z = -50$ m is immobile.

Figure 4 shows the solution (5.24) with $K = (1/800)\text{m}^2\,\text{s}^{-2}$ (corresponding to geostrophic turbulence with 5 cm s^{-1} RMS currents). Now the dispersion of the NIO into the deeper ocean is much faster. In particular, the level of maximum shear propagates downwards at a rate which is roughly in accord with observations. The level of maximum shear reaches about 400 m in 21 days. The main point here is that the final term in (5.21) greatly increases the vertical propagation rate of NIOs.

6. Conclusion and discussion

The dynamics of near-inertial oscillations propagating through a three dimensional geostrophic flow are concisely described by the NIO-equation, (3.2). When the geostrophic flow has a vertical scale larger than the vertical scale of the NIOs then one can use the simpler, alternative formulation in (4.5). These approximations are based only on the assumption that the wave frequency is close to the inertial frequency. In (3.2) and (4.5) there is no requirement that the horizontal length scale of the NIOs be either large or small relative to that of the geostrophic eddies.

As an application of this reduced description of NIO dynamics, we examined the propagation of NIOs through a field of small scale, barotropic, geostropic eddies. It is at this point that we find it useful to introduce an additional spatial-scale separation assumption. The problem is then one of averaging over eddy scales to obtain a mean field description.

Because the geostrophic eddies have a smaller length scale than that of the waves, the spatial structure forced by the eddy vorticity is averaged by the horizontal dispersion of NIOs. This averaging effect is clear in the strong dispersion approximation (5.9): the wavefield expresses the eddy length scales through the eddy streamfunction, which is a low pass filtered version of the eddy vorticity. Because of this averaging, Kunze's (1985) spatially local (in the WKB sense) $\nabla^2\Psi/2$ frequency shift is not directly expressed in the wave field: positive and negative values of $\nabla^2\Psi/2$ cancel because the NIO samples an area which is large relative to the coherence scale of the geostrophic vorticity. There is a rectified effect of the geostrophic eddies: this is the qualitatively new term, $i\overline{\nabla\Psi \cdot \nabla\Psi} L^2 A/2f_0$, which appears in the mean field equation after averaging over the eddy scales—see (5.17).[7]

One remarkable consequence of the new term in (5.17) is that NIOs with infinite horizontal scale (i.e., $k^2 + l^2 = 0$) now disperse vertically. We have argued that this mechanism moves near inertial shear from the mixed layer into the deeper ocean on a time scale of days. This result relies on the strong dispersion approximation and so it must be regarded as suggestive, rather than conclusive. It is intriguing that the strength of these effects is directly proportional to the spatially averaged eddy kinetic energy density. Further, at the level of the strong dispersion approximation, the average kinetic energy density is the only eddy quantity that matters. Thus, there is a link between the grossest aspects of mesoscale turbulence and the processes which might be responsible for mixing the upper ocean.

Acknowledgments. We thank Eric D'Asaro, Paola Cessi, Eric Kunze, Peter Niiler and Dan Rudnick for advice and comments during the course of this research. This research was supported by the National Science Foundation award OCE-9616017.

7. It is instructive to contrast (5.17) with the analogous mean field equation for passive real scalar, (5.4). The result of averaging over the eddy scales is the eddy diffusivity, κ_e. This is not a qualitatively new term in the tracer equation, but merely an augmented version of a term which was already present in the unaveraged advection-diffusion equation, (5.3).

APPENDIX A

Calculation of the leading order pressure

The leading order pressure, p_0 in (2.21), could be obtained from (2.22) if we knew how to determine the constant of integration. This question is related to the elimination of the secular terms in the vertical average of (2.23). We use the notation

$$\overline{\theta} \equiv \frac{1}{H}\int_{-H}^{0} \theta \, dz \tag{A1}$$

to denote a vertical average (H is depth of the ocean). Requiring that all of the terms proportional to e^{-it} in $\overline{R_0}$ cancel gives

$$2\overline{P}_{\xi^*} = \overline{\frac{\partial(B, M)}{\partial(x, y)}} + 2i(\overline{MB_{\xi^*}})_{\xi}. \tag{A2}$$

Given M and B, the equation above can always be solved for $\overline{P}$. For instance, applying ∂_ξ produces $\nabla^2\overline{P} = \text{RHS}$. Thus the real and imaginary parts of $\overline{P}$ satisfy Poisson's equation. Once $\overline{P}$ is obtained from (A2), Eq. (2.22) unambiguously determines the leading order pressure, p_0.

APPENDIX B

A multiple length-scale expansion

We assume that Ψ is barotropic and steady and use (4.5) as a point of departure. Nondimensional variables are defined as:

$$(x, y) = l(\hat{x}, \hat{y}), \qquad z = \lambda_V \hat{z}, \qquad t = l^2\hat{t}/\Psi_0, \tag{B1}$$

where l is the horizontal length scale of the eddies: see (5.2). If $\hat{N}(\hat{z}) = N(z)/N_0$ is the nondimensional buoyancy frequency, then the nondimensional version of the differential operator L is $L = (f_0/N_0\lambda_V)^2\hat{L}$ where:

$$\hat{L} = \partial_{\hat{z}}\hat{N}^{-2}\partial_{\hat{z}}. \tag{B2}$$

Define

$$\hat{\Psi} \equiv \frac{\Psi}{\Psi_0}, \qquad \hat{\beta} = \frac{\beta l^3}{\Psi_0}. \tag{B3}$$

With this notation, the nondimensional version of (4.5) is

$$\mu\Upsilon^{(1)}\left[\hat{L}A_{\hat{t}} + \frac{\partial(\hat{\Psi}, \hat{L}A)}{\partial(\hat{x}, \hat{y})} + i\left(\hat{\beta}\hat{y} + \frac{1}{2}\hat{\nabla}^2\hat{\Psi}\right)\hat{L}A\right] + \frac{i}{2}\hat{\nabla}^2 A = 0. \tag{B4}$$

where $\Upsilon \equiv \Psi f_0/N^2\lambda_V^2$ is the nondimensional parameter discussed in (5.13) and (5.14). $\Upsilon = \mu\Upsilon^{(1)}$, where μ is the scale separation parameter in (5.2). The strong dispersion approximation is implemented by holding $\Upsilon^{(1)}$ fixed as $\mu \to 0$. We now lighten notation by dropping all the hats on dimensionless variables.

The slow space and time scales are

$$(X, Y, T) \equiv \mu(x, y, t). \tag{B5}$$

The multiple scale expansion supposes that Ψ depends only on the fast variables, (x, y, t), while A depends on both the fast variables, and also the slow variables, (X, Y, T). Differential operators acting on A must be expanded with

$$\partial_x \to \partial_x + \mu\partial_X, \qquad \partial_y \to \partial_y + \mu\partial_Y, \qquad \partial_t \to \partial_t + \mu\partial_T. \tag{B6}$$

The fast structure of Ψ can be smoothed out with a spatial average, denoted by an overbar, so that

$$\overline{\Psi} = 0, \qquad \overline{\Psi\nabla^2\Psi} = -\overline{\nabla\Psi\cdot\nabla\Psi}. \tag{B7a, b}$$

Because Ψ depends only on fast variables, $\Psi_X = \Psi_Y = 0$. Finally, we set $\beta = \mu^2\beta_2$ as $\mu \to 0$.

Introducing the scalings above into (5.14) and organizing in powers of μ we have

$$\begin{aligned}\frac{i}{2}\nabla_*^2 A = &-\mu\Upsilon^{(1)}LA_t - \mu\Upsilon^{(1)}\frac{\partial(\Psi, LA)}{\partial(x,y)} - \mu\frac{i}{2}\Upsilon^{(1)}\nabla_*^2\Psi LA - i\mu(A_{xX} + A_{yY})\\ &- \mu^2\Upsilon^{(1)}LA_T - \mu^2\Upsilon^{(1)}[\Psi_x LA_Y - \Psi_y LA_X] - \mu^2 i\Upsilon^{(1)}\beta_2 YLA - \mu^2\frac{i}{2}(A_{XX} + A_{YY}).\end{aligned} \tag{B8}$$

In (B8), $\nabla_*^2 = \partial_x^2 + \partial_y^2$ is the Laplacian of the fast variables only. Now expand A in powers of μ: $A = A_0 + \mu A_1 + \ldots$

The leading order term in (B8) is

$$\frac{i}{2}\nabla_*^2 A_0 = 0. \tag{B9}$$

The solution of (B9) is that

$$A_0 = A_0(X, Y, z, t, T). \tag{B10}$$

Thus, the leading order part of A has no structure on the fast space scales.

Collecting terms of order μ from (B8) we have

$$\frac{i}{2}\nabla_*^2 A_1 = -\Upsilon^{(1)}LA_{0t} - \frac{i}{2}\Upsilon^{(1)}\nabla_*^2\Psi LA_0. \tag{B11}$$

Averaging (B11), and using $\overline{\nabla_*^2 A_1} = \overline{\nabla_*^2\Psi} = 0$, we conclude that $\Upsilon^{(1)}LA_{0t} = 0$. This condition is satisfied by demanding that A_0 in (B10) have no dependence on the fast time t.

The solution of (B11), obtained by cancelling the Laplacian, is then

$$A_1 = -\Upsilon^{(1)}\Psi L A_0. \tag{B12}$$

The first dependence of A on the fast variables (x, y, t) occurs because A_1 in (B12) is proportional to $\Psi(x, y)$. The result in (B12) is recapitulating our earlier heuristic arguments which led to (5.9).

Collecting terms of order μ^2 from (B8) we have

$$\begin{aligned}\frac{i}{2}\nabla_*^2 A_2 = &-\Upsilon^{(1)} L A_{1t} - \Upsilon^{(1)}\frac{\partial(\Psi, LA_1)}{\partial(x, y)} - \frac{i}{2}\Upsilon^{(1)}\nabla_*^2\Psi L A_1 - i(A_{1xX} + A_{1yY}) \\ &- \Upsilon^{(1)} L A_{0T} - \Upsilon^{(1)}[\Psi_x L A_{0Y} - \Psi_y L A_{0X}] - i\Upsilon^{(1)}\beta_2 Y L A_0 - \frac{i}{2}(A_{0XX} + A_{0YY}).\end{aligned} \tag{B13}$$

Averaging (B13),

$$\Upsilon^{(1)} L A_{0T} + i\Upsilon^{(1)}\beta_2 Y L A_0 + \frac{i}{2}(A_{0XX} + A_{0YY}) - \frac{i}{2}\Upsilon^{(1)2}\overline{\Psi\nabla_*^2\Psi}L^2 A_0 = 0. \tag{B14}$$

The final term on the left-hand side of (B14), involving L^2A_0, arises because the term

$$\Upsilon^{(1)}\nabla_*^2\Psi L A_1 = -\Upsilon^{(1)2}\Psi\nabla_*^2\Psi L^2 A_0 \tag{B15}$$

in (B13) has a nonzero spatial average.

The simplifying assumption that $\Psi_z = 0$ has been used at several points in passing from (B13) to (B14). For instance, if $\Psi_z = 0$, then $\partial(\Psi, LA_1)/\partial(x, y) = 0$. And $LA_1 = -\Upsilon^{(1)}\Psi L^2 A_0$. All of these are nonessential simplifications and it is not very difficult to extend the calculation to capture the additional terms which arise if the geostrophic flow is not barotropic. Restoring the dimensions to (B14), and using (B7b), we obtain (5.17).

REFERENCES

Bretherton, F. P. and C. J. R. Garrett. 1968. Wavetrains in inhomogeneous moving media. Proc. Roy. Soc. London, *A302*, 529–554.

D'Asaro, E. A. 1989. The decay of wind forced mixed layer inertial oscillations due to the β-effect. J. Geophys. Res., *94*, 2045–2056.

—— 1995a. Upper-ocean inertial currents forced by a strong storm. Part II: Modeling. J. Phys. Oceanogr., *25*, 2937–2952.

—— 1995b. Upper-ocean inertial currents forced by a strong storm. Part III: Interaction of inertial currents and mesoscale eddies. J. Phys. Oceanogr., *25*, 2953–2958.

D'Asaro, E. A., C. C. Eriksen, M. D. Levine, P. Niiler, C. A. Paulson and P. van Meurs. 1995. Upper-ocean inertial currents forced by a strong storm. Part I: Data and comparisons with linear theory. J. Phys. Oceanogr., *25*, 2909–2936.

Gill, A. E. 1984. On the behavior of internal waves in the wakes of storms. J. Phys. Oceanogr., *14*, 1129–1151.

Klein, P. and A. M. Treguier. 1995. Dispersion of wind-induced inertial waves by a barotropic jet. J. Mar. Res., *53*, 1–22.

Kloosterziel, R. C. and P. Müller. 1995. Evolution of near-inertial waves. J. Fluid Mech., *301*, 269–294.

Kunze, E. 1985. Near inertial wave propagation in geostrophic shear. J. Phys. Oceanogr., *15*, 544–565.

—— 1996. Blocking of near-inertial waves by vertical shear. EOS Trans., *76*, 206.

Moffatt, H. K. 1983. Transport effects associated with turbulence with particular attention to the influence of helicity. Rep. Prog. Phys., *46*, 621–664.

Mooers, C. N. K., 1975a. Several effects of a baroclinic current on the cross-stream propagation of inertial-internal waves. Geophys. Fluid Dyn., *6*, 245–275.

—— 1975b. Several effects of baroclinic currents on the three-dimensional propagation of inertial-internal waves. Geophys. Fluid Dyn., *6*, 277–286.

Pollard, R. T. 1970. On the generation by winds of inertial waves in the ocean. Deep-Sea Res., *17*, 795–812.

Rhines, P. B. 1986. Lectures on ocean circulation dynamics, *in* Large-Scale Transport Processes in Oceans and Atmospheres, J. Willebrand & D. L. T. Anderson eds., D. Reidel Publishing Company.

Rubenstein, D. H. and G. O. Roberts. 1986. Scattering of inertial waves by an ocean front. J. Phys. Oceanogr., *16*, 121–131.

van Meurs, P. 1997. Interactions between near-inertial mixed layer currents and the mesoscale: The importance of spatial variabilities in the vorticity. J. Phys. Oceanogr., (submitted).

Wang, D. P. 1991. Generation and propagation of inertial waves in the subtropical front. J. Mar. Res., *49*, 619–663.

Weller, R. A. 1982. The relation of near-inertial motions observed in the mixed layer during the JASIN (1978) experiment to the local wind stress and to the quasigeostrophic flow field. J. Phys. Oceanogr., *12*, 1122–1136.

Received: *18 November, 1996;* revised: *11 March, 1997.*